วิศวกรรมสาร มข. ปีที่ 32 ฉบับที่ 4 (479 - 501) กรกฎาคม - สิงหาคม 2548
KKU Engineering Journal Vol. 32 No. 4 (479 - 501) July – August 2005

วงจรอินทิเกรเตอร์โหมดกระแสแบบใช้อุปกรณ์แอคทีฟ : บล็อควงจรแอคทีฟสำหรับวงจรประมวลผลสัญญาณอนาลอกในโหมดกระแส *

ทัตยา ปุคคละนันทน์ [1] วรพงศ์ ตั้งศรีรัตน์ [2] และ วัลลภ สุระกำพลธร [3]

[1] อาจารย์ ภาควิชาเทคโนโลยีไฟฟ้าอุตสาหกรรม คณะวิศวกรรมศาสตร์ สถาบันเทคโนโลยีพระจอมเกล้าพระนครเหนือ จังหวัดกรุงเทพฯ 10800

[2] รองศาสตราจารย์ ภาควิชาวิศวกรรมระบบควบคุม คณะวิศวกรรมศาสตร์ สถาบันเทคโนโลยีพระจอมเกล้าเจ้าคุณทหารลาดกระบัง จังหวัดกรุงเทพฯ 10520

[3] ศาสตราจารย์ ภาควิชาอิเล็กทรอนิกส์ คณะวิศวกรรมศาสตร์ สถาบันเทคโนโลยีพระจอมเกล้าเจ้าคุณทหารลาดกระบัง จังหวัดกรุงเทพฯ 10520

Email : ktworapo@kmitl.ac.th

บทคัดย่อ

บทความนี้เป็นการนำเสนอเทคนิคการออกแบบวงจรอินทิเกรเตอร์โหมดกระแสแบบใช้อุปกรณ์แอคทีฟเป็นหลักโดยปราศจากการใช้อุปกรณ์พาสซีฟจากภายนอก วงจรอินทิเกรเตอร์ที่นำเสนอขึ้นประกอบด้วยบล็อควงจรแอคทีฟพื้นฐานเพียงสองชนิดเท่านั้น คือ วงจรทรานสคอนดัคเตอร์กับออปแอมป์ และยังได้นำเสนอการนำไปประยุกต์ใช้งานในวงจรสำหรับสังเคราะห์อนาลอกฟังก์ชันโหมดกระแสต่างๆ เช่น วงจรกรองสัญญาณแลดเดอร์แบบ Leapfrog วงจรกรองสัญญาณไบควอดราทิกที่ปรับค่าได้ทางอิเล็กทรอนิกส์ วงจรสังเคราะห์ฟังก์ชันอิมพีแดนซ์ หลักการดังกล่าวมีความเหมาะสมอย่างมากกับรูปแบบการนำไปออกแบบสร้างเป็นวงจรรวม ในที่นี้ได้ทดสอบและยืนยันสมรรถนะในการทำงานของวงจรที่ได้ออกแบบตามเทคนิคที่นำเสนอด้วยผลการเลียนแบบการทำงานของวงจรด้วยโปรแกรม PSPICE

คำสำคัญ: วงจรอินทิเกรเดอร์ , วงจรโหมดกระแส , วงจรแบบใช้อุปกรณ์แอคทีฟเป็นหลัก ,ออปแอมป์ , โอทีเอ

---

* รับต้นฉบับเมื่อวันที่ 3 พฤศจิกายน 2547 และได้รับบทความฉบับแก้ไขเมื่อวันที่ 13 ธันวาคม 2547

Active-only current-mode integrator : A building block for current-mode analog signal processing circuits *

Tattaya Pukkalanun [1] Worapong Tangsrirat [2] andWanlop Surakampontorn [3]

[1] Lecturer, Department of Industrial Electrical Technology (IET), Faculty of Engineering, King Mongkut's Institute of Technology North Bangkok, Bangkok 10800
[2] Associate Professor, Department of Control Engineering, Faculty of Engineering, King Mongkut's Institute of Technology Ladkrabang, Bangkok 10520
[3] Professor, Department of Electronics, Faculty of Engineering, King Mongkut's Institute of Technology Ladkrabang, Bangkok 10520

Email : ktworapo@kmitl.ac.th

Abstract

A generalized method for designing the continuous-time current-mode integrator, without the use of external passive elements, is proposed in this paper. The integrator is composed only of two fundamental circuit building blocks: a transconductor (g_m) and an internally compensated type operational amplifier. Approaches to realize current-mode network functions: leapfrog ladder filters, an electronically tunable biquadratic filter, and driving-point impedance functions, are presented. Since the approaches are based on the combination of the integrator and transconductane elements, it convenient and suitable for integrated circuit implementation with systematic design and dense layout. The validity of the proposed design approach has been demonstrated by the PSPICE simulation results.

Keywords: Integrator, current-mode circuit, active-only, Operational Amplifier (OA), Operational Transconductance Amplifier (OTA)

---

* Original manucript submitted: November 3, 2004 and Final manucript received: December 13, 2004

Introduction

Because of the main featuring of wider bandwidth, greater linearity, wider dynamic range and simple circuitry compared with their voltage-mode counterparts, at present, current-mode signal processing circuits have received growing interest. Many designs for current-mode analog circuits using high performance active devices, such as, operational amplifier (OA), operational transconductance amplifier (OTA) and second generation current conveyor (CCII), have been investigated and reported [Robert and Sedra. 1992, Higashimura. 1993 and Wu.1994.]. Recently, there is a considerable interest in the design of signal-processing circuits that use only active devices. This is due to the fact that they are more suitable for integrated circuit (IC) fabrication and for high frequency operation [Mitra and Aatre. 1976 and Kumar, and Shukla. 1990]. This design approach utilizes the properties of the finite and complex gain nature of an internally compensated type operational amplifier (ICOA), and the highly linear tunability and a wide tunable range of OTAs. Several implementations for continuous-time signal processing circuits using only active components, are reported in the literature [Abuelma'atti, and Alzaher. 1997, Singh, and Senani. 1998, Tsukutani. Higashimura. Sumi, and Fukui. 2000 and sukutani. Higashimura. Sumi, and Fukui.2000]. Although, they have been demonstrated that the realizations of the resistor-less and the capacitor-less active-only circuits would be attractive for simplicity, integratability, programmability and wide frequency range of operation. However, a design approach that is efficient in terms of systematic design and that is suitable for a very large scale integration (VLSI) has not yet been reported. More over, it is well accepted that OA and transconductance elements are the important circuit building blocks in the design of discrete and analog circuits, such as switched-capacitor and g_m-C circuits [Schaumann. Ghausi and Laker.1990 and Kardontchik. 1992]. Many good realization schemes of the OA and the transconductance element are available in the literatures and in the commercial, both in bipolar and CMOS technologies. Therefore, the implementation in such a way that employs ICOA and transconductance element (g_m) as standard cells will not only be easily constructed from readily available cells, but also significantly simplified the design and layout.

The work of this paper deals with an alternative approach for the realization of an active-only current-mode integrator, which composed only of the transconductance elements and the ICOA, and requires no external passive element. For the case that the transconductance element is realized through the use of a bipolar based OTA, the integrator features an electronically current-gain-tuning property and a temperature-compensated capability. Based on the proposed integrator, a synthesis technique for a leapfrog current-mode ladder filter, which is a general low sensitivity structure, using all-active elements is then presented. The obtained feature of the filter is able to adjust the characteristic of the current transfer functions by electronic means. The realizations of current-mode biquadratic filter and driving-point impedance functions are also outlined. Detail analyses are given as well as simulation results, as examples, being performed with a commercially available LM741 type IC OA and a CA3080 type IC OTA.

Basic circuit building blocks

In the following sections, the circuit elements that are used for the realization of the current-mode circuits in this work will be outlined. The first two circuit elem circuits, are a transconductor and an ICOA. An integrator, which is one of the important circuit ents, which are commonly available and are usually used for the design of voltage–mode building blocks in analog circuit design, realization scheme that without using external passive element is then proposed. The non-idealities of the active-only integrator are also discussed.

A Transconductance Element

A transconductance element or a transconductor is a voltage-controlled current source (VCCS) and is one of the fundamental circuit building blocks to realize electronic circuit elements. Figure 1 shows the circuit models and the symbolic representations of linear transconductors, where the Figure 1(b) is the positive transconductor and the Figure1(d) is the negative transconductor. Generally, to implement the transconductors of Figure 1, the available transconductance elements, such as the bipolar-based, the CMOS-based and GaAs-based structures, can be employed, depending on the technology that the designer working on. However, in this paper, without loss of generality and for the simplicity and compatibility with bipolar technology, a simple bipolar structure such an operational transconductance amplifier (OTA) as shown in Figure 2 will be chosen. For this structure, if V_T is the thermal voltage, the OTA transconductance gain g_m can be given by

$$g_m = \frac{I_B}{2V_T} \tag{1}$$

It is indicated that, for the bipolar-based OTA, the value of g_m can be linearly and electronically tuned by changing the external bias current I_B.

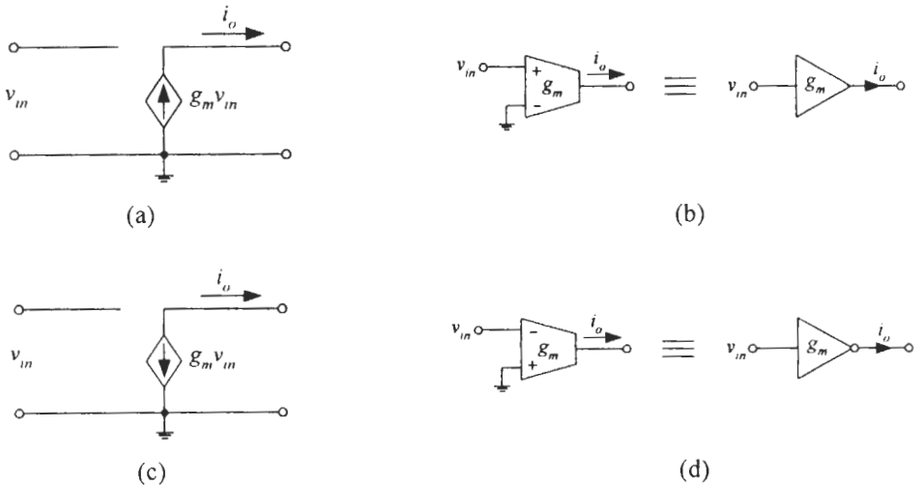

Figure1 *Transconductance elements*
for positive g_m : (a) circuit model (b) symbolic representation, $i_o = g_m v_{in}$
for negative g_m : (c) circuit model (d) symbolic representation, $i_o = -g_m v_{in}$

An Internally Compensated Type OA

The amplifier used in this realization is an ICOA, which its model and the symbolic representation are shown in the Figure .3. It is assumed that the amplifier has a finite open-loop frequency-dependent gain. If ω_a is the –3 dB bandwidth and by considering for the frequencies of $\omega >> \omega_a$, the open-loop gain $A(s)$ of the amplifier will be henceforth characterized by

$$A_V(s) = \frac{V_o}{V_{in}} = \frac{A_o \omega_a}{s + \omega_a} \cong \frac{B}{s} \tag{2}$$

where B denotes the gain-bandwidth product (GBP) of the ICOA in radian per second, which is the product of the open-loop dc gain A_o and the 3-dB bandwidth ω_d. Noting from the equation (2) that the ICOA is functioned as a voltage-mode integrator.

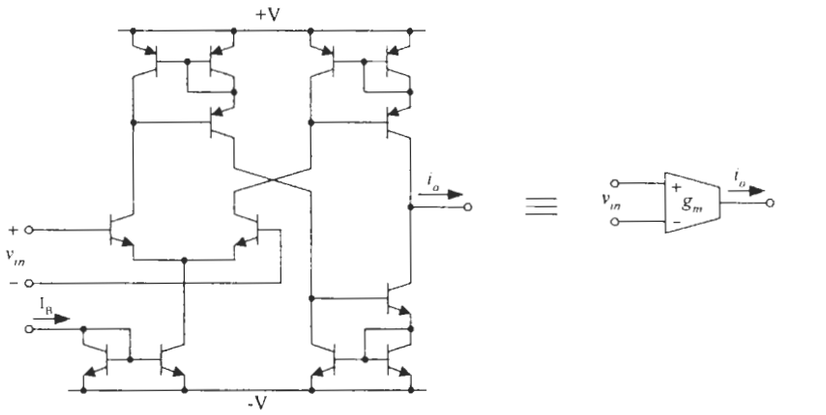

(a) (b)

Figure 2 *Simple bipolar implementation of a transconductance element (a) circuit diagram (b) its symbol*

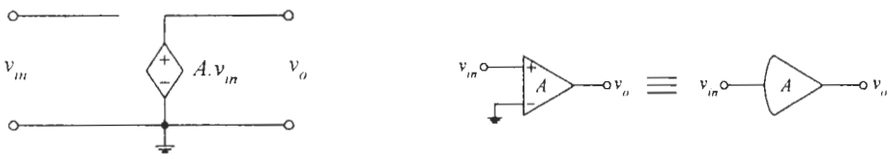

(a) (b)

Figure 3 *Characterization of an internally compensated type operational amplifier (ICOA) (a) circuit model (b) symbolic representation, $v_o = Av_{in}$*

An Active-Only Dual-Output Current-Mode Integrator

The proposed current-mode integrator

In this section, a current-mode integrator that is constructed from the transconductance elements and the ICOA of the previous sections is introduced and its performance is also discussed. Figure 4 shows the schematic diagram and symbolic representation of the proposed current-mode dual-output integrator that without using external capacitor, where the dual-current-output OTA has been implemented using single-ended OTAs in the parallel connection [Wu. 1994]. The integrator provides both the positive and negative output currents. Noting that both the dual-output integrator and the single-output integrator are used in this paper. From routine circuit analysis, the current transfer function of the integrator can be given as:

$$A_I(s) = \frac{I_o(s)}{I_{in}(s)} = \frac{B}{s}\left[\frac{g_{m2}}{g_{m1}}\right] = \frac{B}{s}A_G \qquad (3)$$

where A_G denotes the integrator gain, which is the ratio between the transconductance gains g_{m2} and g_{m1}. Due to that, for the ordinary bipolar-based OTA of Fig.2, the transconductance gains $g_{m1} = I_{B1}/2V_T$ and $g_{m2} = I_{B2}/2V_T$, where I_{B1} and I_{B2} are the bias currents of the first and the second OTAs, respectively. Thus, equation (3) becomes

$$A_I(s) = \frac{I_o(s)}{I_{in}(s)} = \frac{B}{s}\left[\frac{I_{B2}}{I_{B1}}\right] = \frac{B}{s}A_G \tag{4a}$$

Now the current gain A_G is the bias current ratio between I_{B2} and I_{B1} or

$$A_G = \frac{I_{B2}}{I_{B1}} \tag{4b}$$

From equations (1) and (4b), one can see that the temperature dependence of the transconductance gains g_{m1} and g_{m2} of the OTAs are compensated. This means that if the ordinary bipolar-based OTAs are employed, the integrator is less sensitive to temperature.

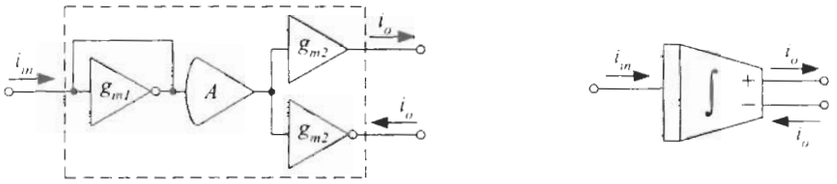

Figure 4 *The proposed active-only current-mode dual-output integrator (a) circuit diagram (b) its symbol*

Non-ideal performance

Deviation from the ideal performance, that predicted in the equations (3) and (4), is due to the parasitic effects of the non-ideality characteristics of the ICOA and the OTA. If the parasitic pole of the ICOA is taken into consideration, the open-loop voltage gain $A_V(s)$ can be expressed as

$$A_V(s) = \frac{B}{s}\frac{\omega_b}{(s+\omega_b)} = \frac{B}{s}\frac{1}{(1+\tau_b s)}$$

where $\omega_b = 1/\tau_b$ and ω_b is the second dominant pole of the ICOA, where in general $\omega_b \cong 1$ MHz. The open-loop gain $A_V(s)$ can now be rewritten as

$$A_V(s) \cong \frac{B}{s}\left(1 - \frac{s}{\omega_b}\right) \tag{5}$$

For the transconductor, let $\omega_c = 1/\tau_c$ represents the transconductor internal-pole, where usually $\omega_c \cong 2$ MHz and g_{m0} is the low frequency transconductance gain. The open-loop transconductance gain $g_m(s)$ for general case can be described by

$$g_m(s) = \frac{g_{m0}}{\left(1 + \frac{s}{\omega_c}\right)} \cong g_{m0}\left(1 - \frac{s}{\omega_c}\right) \tag{6}$$

Therefore, the frequency response of the current-mode integrator in Figure 4 that including the second dominant pole of the ICOA and the transconductor internal-poles can now be given by

$$\frac{I_o(s)}{I_{in}(s)} = \left[\frac{B}{s}\right]\left[1 - \frac{s}{\omega_b}\right]\left[\frac{g_{m02}\left(1 - \frac{s}{\omega_{c2}}\right)}{g_{m01}\left(1 - \frac{s}{\omega_{c1}}\right)}\right] \tag{7}$$

where ω_{c1} and ω_{c2} are the effective transconductance element internal-poles of the first and second transconductors, respectively. Equation (7) can also be rewritten as:

$$\frac{I_o(s)}{I_{in}(s)} = \left[\frac{B}{s}\right]\left[1 - \frac{s}{\omega_b}\right]\left[\frac{I_{B2}}{I_{B1}}\right]\left[\frac{\omega_{c2} - s}{\omega_{c2}}\right]\left[\frac{\omega_{c1}}{\omega_{c1} - s}\right] \tag{8}$$

For implemented in monolithic integrated circuit form, we can expect the transconductors g_{m1} and g_{m2} are matched or $\omega_{c1} \cong \omega_{c2}$. However, if the transconductors g_{m1} and g_{m2} are not matched. We can also see from equation (8) that at the frequencies much lower than ω_{c1} and ω_{c2}, or $\omega << \omega_{c1}$ and $\omega << \omega_{c2}$, equation (8) still becomes frequency independent. Since $A_{ci} = I_{B2}/I_{B1}$ is the integrator dc gain, the current transfer function $A_I(s)$ can be reasonably reduced to

$$A_I(s) = \frac{I_o(s)}{I_{in}(s)} = \left[\frac{A_G B}{s}\right]\left[1 - \tau_b s\right] \tag{9}$$

From equation (9) one can see that the frequency characteristic of the proposed current-mode integrator has a dc current gain equaled to equation (3) and has a high-frequency dominant pole located at ω_b. This pole should be the major high-frequency limitation of the proposed current-mode integrator.

Current-mode filters realization procedures

In order to demonstrate the usefulness, in this section, the proposed active only integrator is employed to realize current-mode filters. Both the two commonly used realization techniques will be considered. The first technique is the realized by using the simulation of the LC ladder prototype. This configuration has been receiving considerable attention and popular due to it shares all the low sensitivity and low component spread of the RLC prototypes. The other technique is the realization of a biquadratic section. The major advantage of this configuration is that multi-functional filter is available in one circuit.

Current-Mode All-Pole Leapfrog Ladder Filters

To illustrate the systematical design procedure using the proposed current-mode integrator, the doubly terminated n^{th}-order all-pole LC ladder low-pass filter prototype as shown in Figure 5 is simulated. The relations of the leapfrog structure for the branches, the meshes and the nodes in this filter are interrelated by :

$$
\begin{aligned}
I_1 &= I_S - \frac{V_1}{R_S} - I_2 \quad , \quad V_1 = \frac{I_1}{sC_1} \\
V_2 &= V_1 - V_2 \quad , \quad I_2 = \frac{V_2}{sL_2} \\
I_3 &= I_2 - I_4 \quad , \quad V_3 = \frac{I_3}{sC_3} \\
&\vdots \quad , \quad \vdots \\
V_j &= V_{j-1} - V_{j+1} \quad , \quad I_j = \frac{V_j}{sL_j} \\
I_i &= I_{i-1} - I_{i+1} \quad , \quad V_i = \frac{I_i}{sC_i} \\
&\vdots \quad , \quad \vdots \\
V_{n-1} &= V_{n-2} - V_n \quad , \quad I_{n-1} = \frac{V_{n-1}}{sL_{n-1}} \\
\text{and} \quad I_n &= I_{n-1} - I_o \quad , \quad V_n = \frac{I_n}{sC_n}
\end{aligned}
\tag{10}
$$

These equations result in a leapfrog structure that using only integrators, multipliers and subtractors that can be shown by the block diagram of Figure 6. Through the use of the active devices as mentioned in the section 2, the circuit diagram thus obtained from the leapfrog realization of Figure 6 can be shown in Figure 7. If we design such that $g_{m1} = g_{m2} = \ldots = g_{mn} = g_m$, then the design equations of the circuit parameters can be expressed as follows :

$$R_S = R_L = R = \frac{1}{g_m} \tag{11a}$$

$$C_1 = \frac{g_m}{A_{G1}B_1} \quad , \quad L_2 = \frac{1}{g_m A_{G2} B_2} \tag{11b}$$

$$C_3 = \frac{g_m}{A_{G3}B_3} \quad , \quad L_4 = \frac{1}{g_m A_{G4} B_4} \tag{11c}$$

$$\vdots \quad , \quad \vdots$$

$$C_i = \frac{g_m}{A_{Gi} B_i} \quad , \quad L_j = \frac{1}{g_m A_{Gj} B_j} \tag{11d}$$

and

$$A_{Gk} = \frac{I_{B2k}}{I_{B1k}} \tag{11e}$$

where (i = 1 , 3 , 5 , ..., n) and (j = 2 , 4 , 6 , ..., n-1) and A_{Gk} and B_k (k = 1, 2, ..., n) represent the current gain of the k-th integrator and the GBP of the k-th ICOA, respectively. Note that all integrators, which simulate the behavior of capacitors and inductors, can be electronically tuned through adjusting the gain parameters of A_{Gk}.

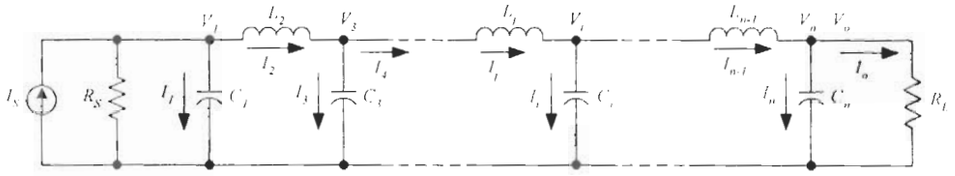

Figure 5 *Current-mode n^{th}-order all-pole LC ladder lowpass prototype*

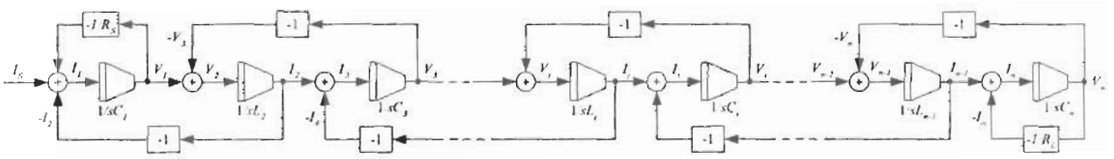

Figure 6 *Block diagram representation of the leapfrog structure of the lowpass filter*

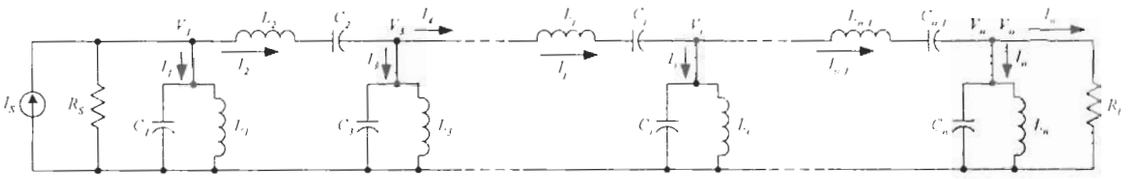

Figure 8 *Current-mode n^{th}-order LC ladder bandpass prototype*

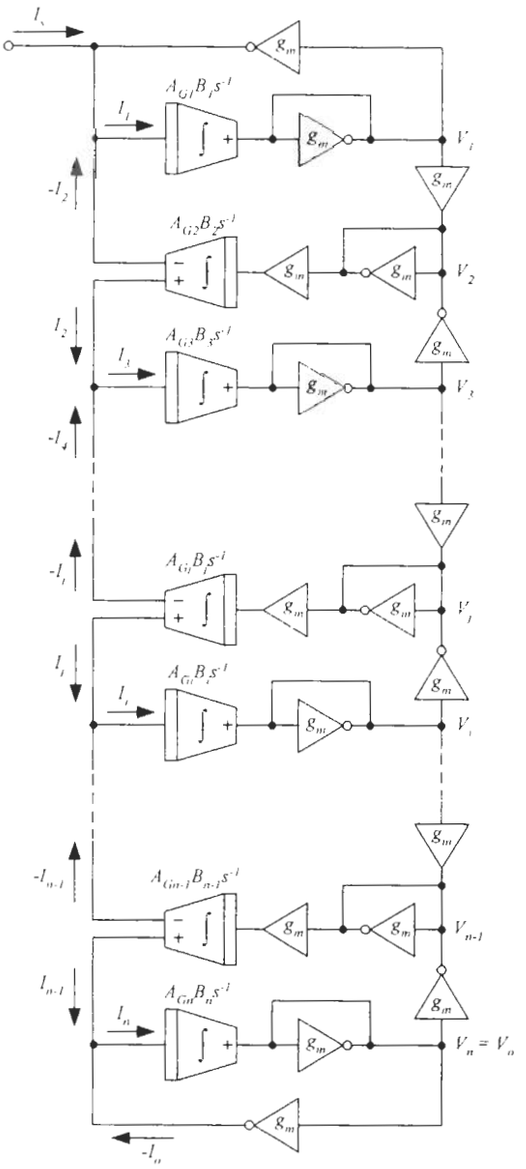

Figure 7 *System diagram for active-only current-mode third-order lowpass filter*

Example 1 : For the design of a current-mode third-order (n = 3) Butterworth lowpass filter by simulation of the passive filter of Figure 5 with a cut-off frequency f_{-3dB} of 100 kHz, the design procedure will be as follows:

(1) If the terminated resistors R_S = R_L = 1 kΩ, this specification leads to the passive elements with the values of : C_1 = C_3 = 1.59 nF and L_2 = 3.185 mH.

(2) From equation (11), for R_S = R_L = 1 kΩ, all g_m values are equal to 1 mS.

(3) Let the ICOAs with $B_1 = B_2 = B_3 = 5.906$ Mrad/s are chosen (Singh and Senani 1998). Thus, by calculating the circuit parameters obtained from the equation (11) yields : $A_{G1} = A_{G3} = 0.106$ and $A_{G2} = 0.053$.

(4) From the obtained current gains and the equation (11e), if we set the bias currents $I_{B11} = I_{B12} = I_{B13} = 1$ mA, then the bias currents $I_{B21} = I_{B23} = 106$ μA and $I_{B22} = 53$ μA.

Current-Mode Bandpass Leapfrog Ladder Filters

Figure 8 shows the doubly terminated n[th]-order LC ladder bandpass network. The simulation can be done by the repeating use of the circuit branches typically consisting of parallel and series combinations of capacitors and inductors. The voltage-current characteristics of these sub-circuits can be derived respectively by:

For the parallel combination branches gives:

$$V_i = Z_C(I_i - Y_L V_i) = \frac{1}{sC_i}\left(I_i - \frac{V_i}{sL_i}\right) \quad ; \text{ for } i = 1, 3, 5, \ldots, n \qquad \textbf{(12a)}$$

and the series combination branches gives:

$$I_j = Y_L(V_j - Z_C I_j) = \frac{1}{sL_j}\left(V_j - \frac{I_j}{sC_j}\right) \quad ; \text{for } j = 2, 4, 6, \ldots, n\text{-}1 \qquad \textbf{(12b)}$$

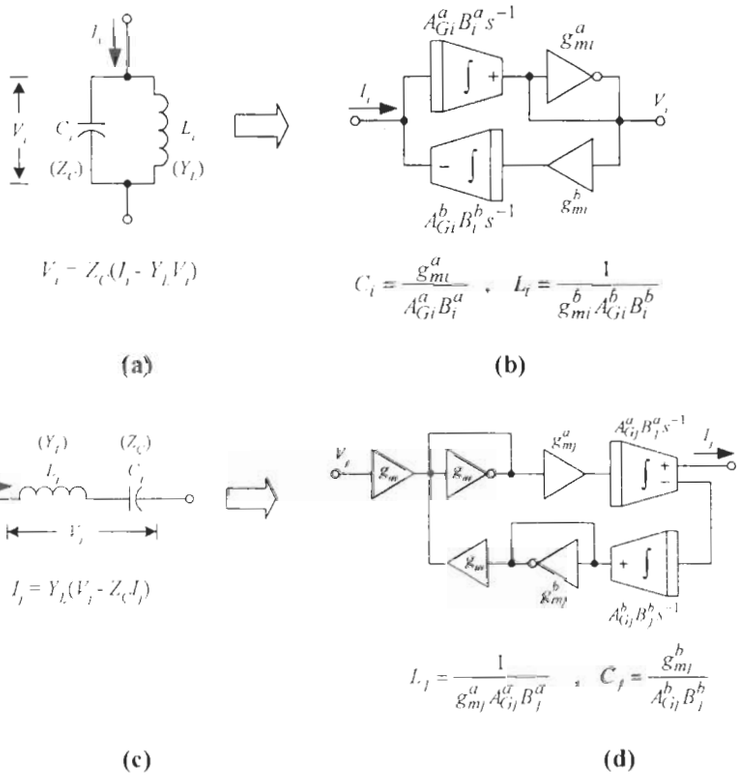

Figure 9 *Sub-circuits of the filter of Fig.8 involving all-active elements*

The active-only implementation of these structures, corresponding to the sub-circuits of Figs. 9(a) and 9(c), are then shown in Figure 9(b) and 9(d), respectively. By choosing $g^a_{mi} = g^b_{mi} = g^a_{mj} = g^b_{mj} = g_m$ (i = 1, 3, 5, ... and j = 2, 4, 6, ...) and by the similar realization procedure as in section 3.1 yields the circuit parameters of each branch in the leapfrog, which can summarize as follows :

$$R_S = R_L = R = \frac{1}{g_m} \tag{13a}$$

$$C_i = \frac{g_m}{A^a_{Gi} B^a_i} \quad , \quad L_i = \frac{1}{g_m A^b_{Gi} B^b_i} \tag{13b}$$

$$C_j = \frac{g_m}{A^b_{Gj} B^b_j} \quad , \quad L_j = \frac{1}{g_m A^a_{Gj} B^a_j} \tag{13c}$$

$$A^a_{Gi} = \frac{I^a_{B2i}}{I^a_{B1i}} \quad , \quad A^a_{Gj} = \frac{I^a_{B2j}}{I^a_{B1j}} \tag{13d}$$

and

$$A^b_{Gi} = \frac{I^b_{B2i}}{I^b_{B1i}} \quad , \quad A^b_{Gj} = \frac{I^b_{B2j}}{I^b_{B1j}} \tag{13e}$$

where usually for integrated circuit we can choose that $B^a_i = B^b_i = B^a_j = B^b_j = B$ (i = 1, 3, 5,... and j = 2, 4, 6,...). Thus, the realization diagram of the bandpass filter based on the sub-circuits of the Fig.9 can be shown in Figure 10.

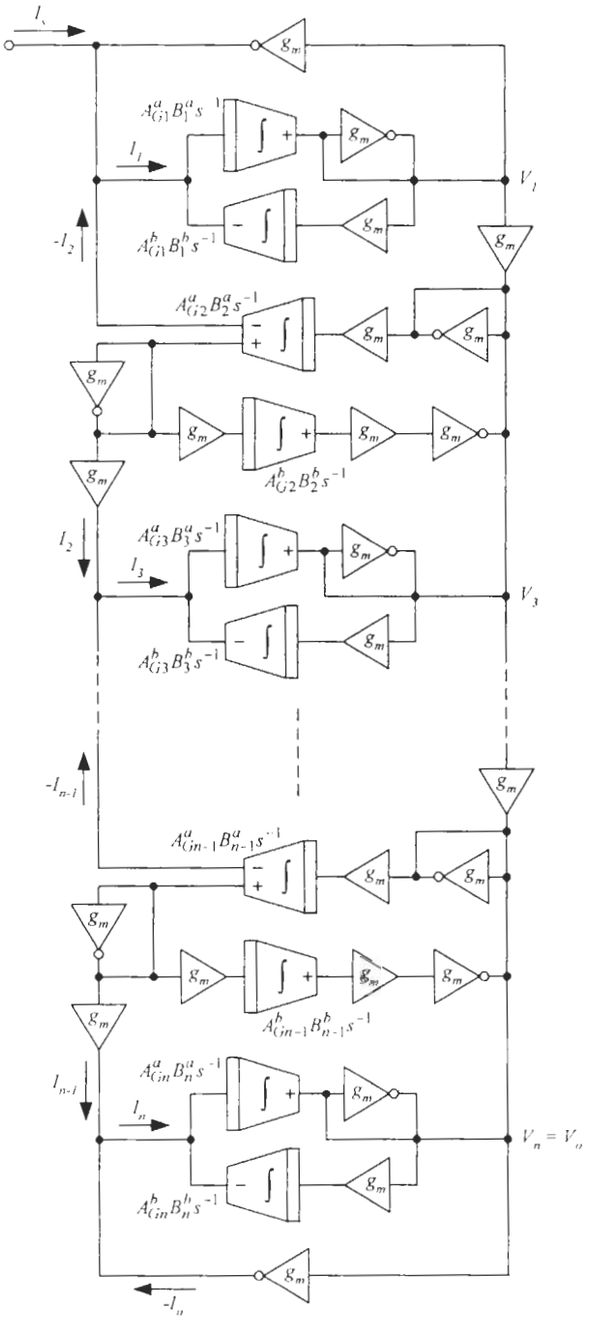

Figure 10 *System diagram for active-only current-mode sixth-order bandpass filter*

Example 2 The design procedure for a sixth-order (n = 6) Chebyshev bandpass filter using Figure 10 for the following specifications: center frequency f_c = 50 kHz, with the bandwidth of 1.0 and the ripple width of 0.5 dB are as follows:

(1) From the specification and for $R_S = R_L = 1$ kΩ, the resulting passive circuit elements are: $R_S = R_L = 1$ kΩ, $C_1 = C_3 = 5.08$ nF, $L_1 = L_3 = 1.99$ mH, $C_2 = 2.90$ nF and $L_2 = 3.49$ mH.

(2) By choosing $R_S = R_L = 1$ kΩ, all the g_m values are equal to 1 mS.

(3) Let we choose the ICOAs with $B_1 = B_2 = B_3 = 5.906$ Mrad/s. Thus, by calculating the circuit parameters obtained from equation (13) yields the gain parameters as : $A^a_{G1} = A^a_{G3} = 0.033$, $A^b_{G1} = A^b_{G3} = 0.085$ and $A^a_{G2} = 0.048$, $A^b_{G2} = 0.058$.

(4) From the obtained current gains and the equation (13d), if we set the bias current $I^a_{B11} = I^a_{B13} = I^b_{B11} = I^b_{B13} = I^a_{B12} = I^b_{B12} = 1$ mA, then the bias currents : $I^a_{B21} = I^a_{B23} = 33$ μA, $I^b_{B21} = I^b_{B23} = 85$ μA, $I^a_{B22} = 48$ μA and $I^b_{B22} = 58$ μA.

Current-Mode Biquadratic Filters

To realize a current-mode biquadratic filter, the block diagram of Figure11(a) [E. Sanchez-Sinencio. R.L. Geiger, and H. Nevarez-Lozano. 1988] will be used as a scheme for deriving the biquadratic functions. The realization of an electronically tunable current-mode biquadratic filter using only active elements is shown in Fig.11(b), with the gains $K_1 = A_{G1}$, $K_2 = A_{G2}$ and $K_3 = g_{mb}/g_{ma}$. Thus, the current transfer functions of this configuration can be given by

$$T_{HP}(s) = \frac{I_{HP}(s)}{I_{in}(s)} = \frac{s^2}{D(s)} \tag{14}$$

$$T_{BP}(s) = \frac{I_{BP}(s)}{I_{in}(s)} = \frac{s\left(\dfrac{g_{mb}A_{G1}B_1}{g_{ma}}\right)}{D(s)} \tag{15}$$

$$T_{LP}(s) = \frac{I_{LP}(s)}{I_{in}(s)} = \frac{A_{G1}A_{G2}B_1B_2}{D(s)} \tag{16}$$

where
$$D(s) = s^2 + s\left(\frac{g_{mb}A_{G1}B_1}{g_{ma}}\right) + \left(A_{G1}A_{G2}B_1B_2\right) \tag{17}$$

It is clearly shown from equations (14)-(17) that the three current transfer functions, i.e., T_{HP} (s) = highpass, T_{BP} (s) = bandpass, T_{LP} (s) = lowpass, are simultaneously available on this configuration. The active filter resonance angular frequency ω_o and quality factor Q can be respectively given by

$$\omega_o = \sqrt{A_{G1}A_{G2}B_1B_2} \tag{18}$$

and
$$Q = \frac{g_{ma}}{g_{mb}}\sqrt{\frac{A_{G2}B_2}{A_{G1}B_1}} \tag{19}$$

From which it can be found that the active sensitivities can be expressed as

$$S_{A_{G1}}^{\omega_o} = S_{A_{G2}}^{\omega_o} = S_{B_1}^{\omega_o} = S_{B_2}^{\omega_o} = \frac{1}{2} \tag{20}$$

$$S_{A_{G1}}^{Q} = -S_{A_{G2}}^{Q} = S_{B_1}^{Q} = -S_{B_2}^{Q} = -\frac{1}{2} \tag{21}$$

and

$$S_{g_{ma}}^{Q} = -S_{g_{mb}}^{Q} = 1 \tag{22}$$

Noting that all the active sensitivity values are less than unity. Furthermore, if we set $A_{G1} = A_{G2} = A_G$ and $B_1 = B_2 = B$, then ω_o and Q-factor from equations (18) and (19) can be rewritten as

$$\omega_o = A_G B \tag{23}$$

and

$$Q = \frac{g_{ma}}{g_{mb}} \tag{24}$$

According to equation (18), it should be mentioned that the natural frequency ω_o can be linearly adjusted by controlling A_G without effecting the Q-factor, whereas the large value of Q-factor is obtainable by properly adjusting through g_{ma} and g_{mb}. Additionally, the temperature dependence of the gains A_G, and g_{ma} and g_{mb} are compensated. Thus, this means that the filter also enjoys orthogonal tuning of the circuit parameters ω_o and Q-factor via the transconductance parameters and it's also temperature independent. The characteristic of the filter will be demonstrated by simulation results in section 5.

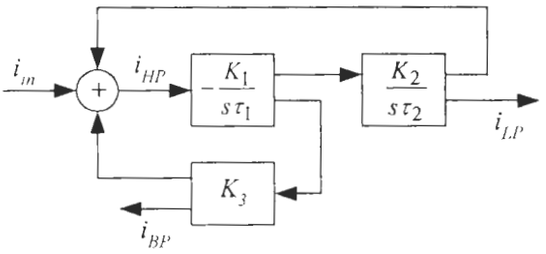

(a)

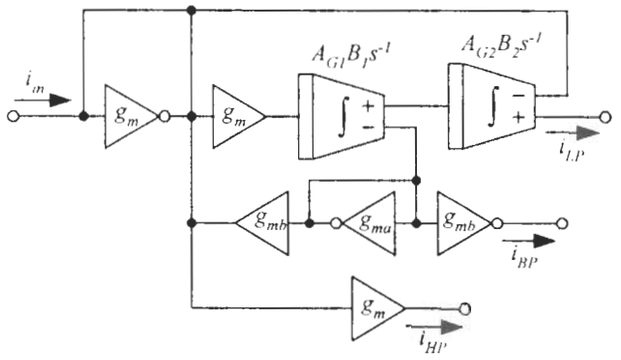

(b)

Figure 11 *Electronically tunable current-mode biquadratic filter (a) block diagram representation (b) structure realization*

Example 3 To design the electronically tunable current-mode biquadratic filter of the Figure 11(b) with $\omega_o/2\pi \cong 50$ kHz at the Q-factor = 1, the procedure can be done as follows :

(1) Since Q =1, from equation (24), we can set $g_{ma} = g_{mb} = 1$ mS.

(2) If the ICOA with $B = 5.906$ Mrad/s is used and $\omega_o/2\pi \cong 50$ kHz, then from equation (23), the current gains $A_{G1} = A_{G2} = A_G = 0.053$. This can be done by setting $I_{B11} = I_{B12} = I_{B13} = 1$ mA and $I_{B21} = I_{B22} = I_{B23} = 53$ μA.

To discuss the non-ideal effect of the proposed integrator on the filter's frequency characteristics, the parasitic second dominant pole of the ICOA from equation (9) is taken into account. As a result, the percentage inaccuracies of the ω_o and Q-factor in this case are respectively found to be

$$\frac{\delta\omega_o}{\omega_o} = \left\{\left[1+\left(A_{G1}B_1\tau_{b1}\right)\left(A_{G2}B_2\tau_{b2}-\frac{g_{mb}}{g_{ma}}\right)\right]^{1/2}-1\right\}\times 100\% \tag{25}$$

and

$$\frac{\delta Q}{Q} = \frac{\left[1-\left(\frac{g_{ma}A_{G2}B_2}{g_{mb}}\right)\left(\tau_{b1}+\tau_{b2}\right)\right]-\left[1+\left(A_{G1}B_1\tau_{b1}\right)\left(A_{G2}B_2\tau_{b2}-\frac{g_{mb}}{g_{ma}}\right)\right]^{1/2}}{\left[1+\left(A_{G1}B_1\tau_{b1}\right)\left(A_{G2}B_2\tau_{b2}-\frac{g_{mb}}{g_{ma}}\right)\right]^{1/2}}\times 100\% \tag{26}$$

where $\omega_{b1} = 1/\tau_{b1}$, $\omega_{b2} = 1/\tau_{b2}$ and ω_{b1} and ω_{b2} are the second dominant poles of the ICOA1 and ICOA2, respectively. It can be found that the undesirable factors, which are yielded by the parasitic effects of ICOAs, can be made negligible if such factors are considered as the condition:

$$1 >> \left(\frac{g_{ma}A_{G2}B_2}{g_{mb}}\right)\left(\tau_{b1}+\tau_{b2}\right) \tag{27}$$

Realizations of driving-point impedance functions

Some more applications of the active-only integrator are outlined in this section. The simulations of driving-point impedance functions, such as, inductors, capacitance multiplier and frequency-dependent negative resistance (FDNR), will be discussed.

Inductance Simulations

Figure 12(a) shows the schematic diagram for the implementation of a tunable grounded inductance simulation using all active devices. From this circuit, it can easily be shown that the driving point impedance is

$$Z_{in}(s) = s\left[\frac{1}{g_m A_G B}\right] \tag{28}$$

where the magnitude of the grounded simulated inductance is

$$L_{eq} = \left[\frac{1}{g_m A_G B}\right] \tag{29}$$

It should be noted that the equivalent inductance L_{eq} could properly be tuned by electronic means through the g_m or A_G. In addition, the circuit in Figure12(a) can easily be modified to simulate a floating inductor by connecting the minus current-output of the integrator as shown in Figure 12(b).

Capacitance Multiplier Simulations

The application of the proposed integrator to simulate a grounded capacitance is shown in the Figure 13(a). The magnitude of the simulated capacitance for this scheme can be given by

$$Z_{in}(s) = \frac{1}{s}\left[\frac{A_G B}{g_m}\right] \tag{30}$$

where the simulated equivalent capacitance is equal to

$$C_{eq} = \left[\frac{g_m}{A_G B}\right] \tag{31}$$

Since the transconductance gain g_m and the integrator gain A_G are electronically variable, the simulated capacitance magnitude will also be electronically variable. The grounded capacitance multiplier of Figure 13(a) can conveniently be converted into a corresponding floating capacitance multiplier by adding an additional transconductance elements as shown in Figure 13(b).

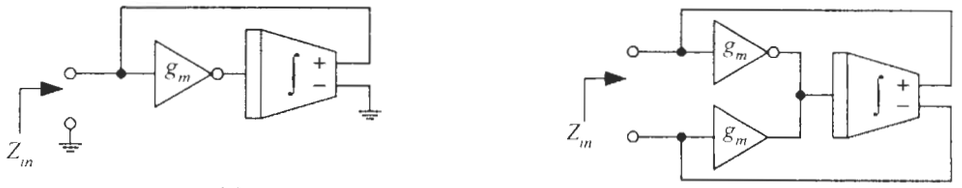

Figure12 *Inductance simulations*
(a) grounded inductor (b) floating inductor

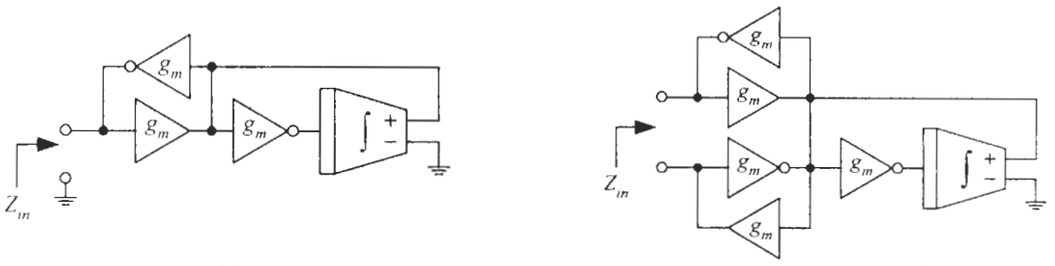

Figure 13 *Capacitance multiplier simulations*
(a) grounded capacitance multiplier (b) floating capacitance multiplier

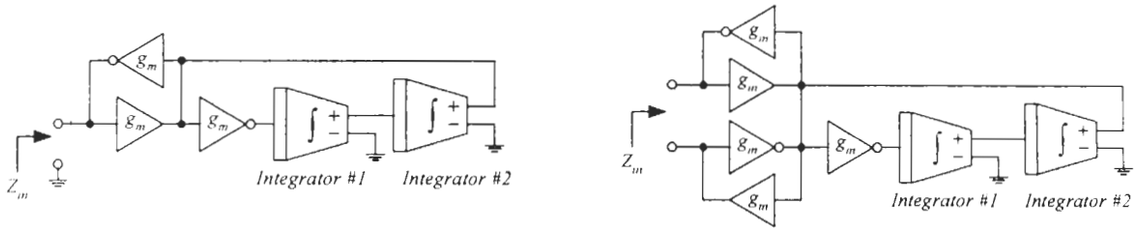

Figure 14 *FDNRs*
(a) grounded FDNR (b) floating FDNR

Frequency-Dependent Negative Resistances (FDNRs)

The scheme diagram for simulating a FDNR element is shown in Fig.14(a). Its analysis gives the driving-point impedance function as follows :

$$Z_{in}(s) = \frac{1}{s^2}\left[\frac{A_{G1}A_{G2}B_1B_2}{g_m}\right] \tag{32}$$

where the circuit behaves as a grounded FDNR element with

$$D = \left[\frac{g_m}{A_{G1}A_{G2}B_1B_2}\right] \tag{33}$$

where A_{Gi} and B_i are the current gain and the ICOA's GPB of i-th integrator unit (i = 1, 2), respectively. In contrast to the conventional circuits, this scheme does not require any external

passive elements and its characteristic can be electronically tuned. In the same manner, Figure 14(b) shows the system diagram for simulating a floating FDNR element.

Simulation results

To verify and study the performances of the proposed integrator and the filters in section 3, PSPICE simulation results are employed. In this simulation, the bipolar-based implementation of transconductance element is modeled by employing CA3080 type OTA (Wu 1994), and the LM741 type ICOA with the gain-bandwidth product B = 5.906 Mrad/s (Singh and Senani 1998). Figure 15 shows the simulated frequency responses of the integrator. The results show that the proposed circuit acts as an integrating function with a slope -20 dB per decade for the frequency range from 10 Hz to 1 MHz and has less than 10% phase error from the frequency range of 30 Hz to 500 kHz.

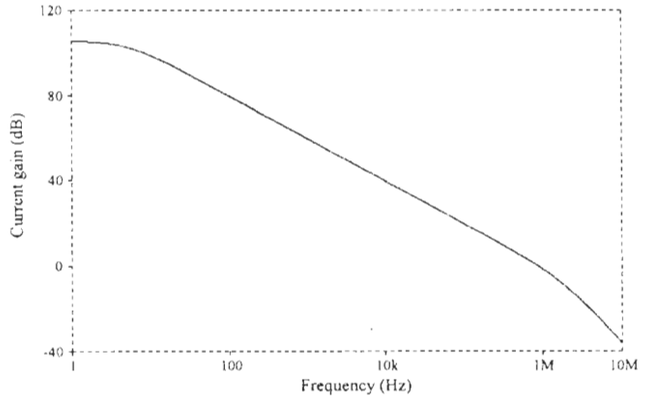

(a)

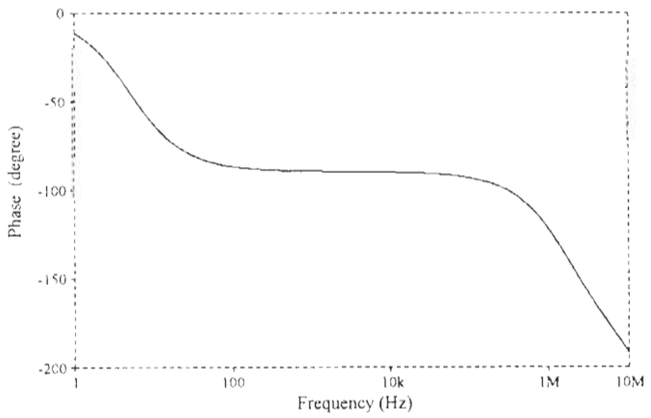

(b)

Figure 15 *Frequency responses of an active-only current-mode integrator*
(a) magnitude of the current transfer function in decibel (b) phase of the current transfer function in degree

Figure 16 shows the performance of the third-order current-mode Butterworth lowpass filter of Fig.7 with the cut-off frequency f_{3dB} of 100 kHz. According to the example 1, the current

gains are set by $A_{G1} = A_{G3} = 106\mu A/1mA$ and $A_{G2} = 53\mu A/1mA$. The simulated frequency response exhibits reasonably close agreement with the ideal response. For the sixth-order Chebyshev bandpass filter of Fig.10 and the example 2, the current gains are set by $A^a_{G1} = A^a_{G3} = 33\mu A/1mA$, $A^b_{G1} = A^b_{G3} = 85\mu A/1mA$ and $A^a_{G2} = 48\mu A/1mA$, $A^b_{G2} = 58\mu A/1mA$. The ideal and simulated responses are shown in Figure 17. It should be noted from the Figure 16 and 17 that the discrepancies appearing above the high frequency of about 1 MHz arise mainly from the effect of the GBP of an ICOA. The simulated frequency responses shown that the frequency characteristic is conveniently variable by tuning the external controlled of the current gains A_G.

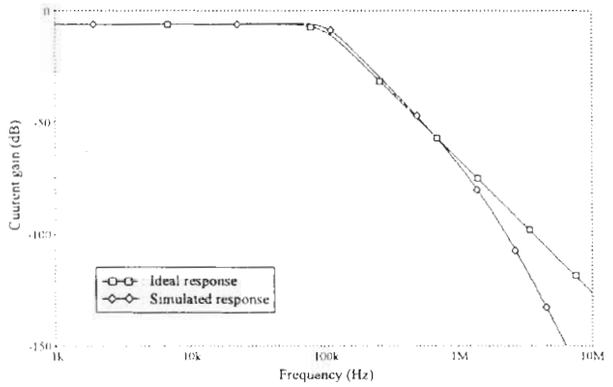

Figure 16 *Ideal and simulated responses of the third-order Butterworth lowpass filter of Figure 7*

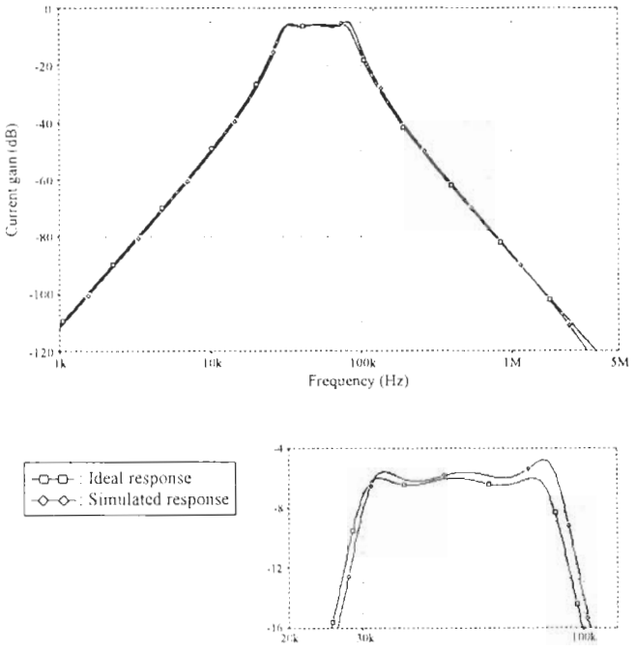

Figure 17*Ideal and simulated responses of the sixth-order Chebyshev bandpass filter of Figure 10*

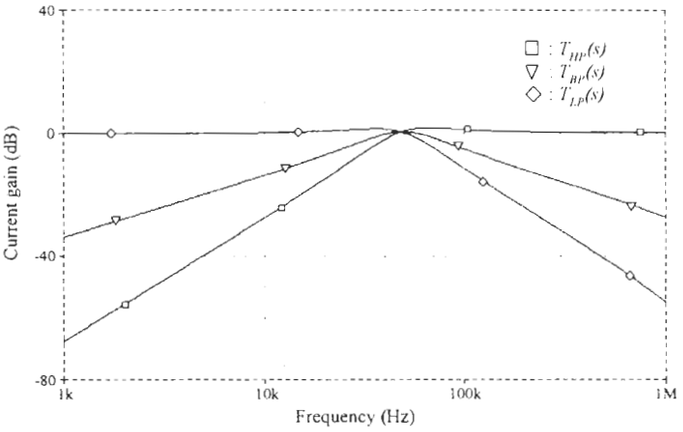

Figure 18 *Simulated responses of highpass, bandpass and lowpass filters*

Figure 18 shows simulated responses of the electronically tunable current-mode biquadratic filter of Figure 11(b), when $A_{G1} = A_{G2} = A_G = 0.053$ and $g_{ma} = g_{mb} = 1$ mS. From the example 3, this filter is designed for $\omega_o/2\pi \cong 50$ kHz and the Q-factor = 1. Figure 19 shows the resultant characteristics for three different values of g_{ma}, i.e., g_{ma} = 0.1 mS, 0.5 mS and 1.0 mS, while g_{mb} = 1 mS and A_G = 0.1, respectively. The following is selected to obtain the Q-factor values are 1, 5, 10, respectively. It is shown that the Q-factor can be electronically controlled through adjusting g_{ma} without disturbing the natural angular frequency ω_o. In order to illustrate the controllability of the ω_o by tuning A_G, the transconductance gains g_{ma} and g_{mb} are set to be constant at 1.0 mS and 0.1 mS, respectively, this following setting is kept Q-factor = 10. The obtained responses of bandpass filters when A_G is varied are shown in Fig.20. The corresponding natural frequencies obtained by simulation are 48.98 kHz, 97.72 kHz and 484.17 kHz, and correspond to theoretical values calculated from equation (23). All the simulated responses shown above imply that the proposed filter should exhibit reasonably good agreement with the presented prediction.

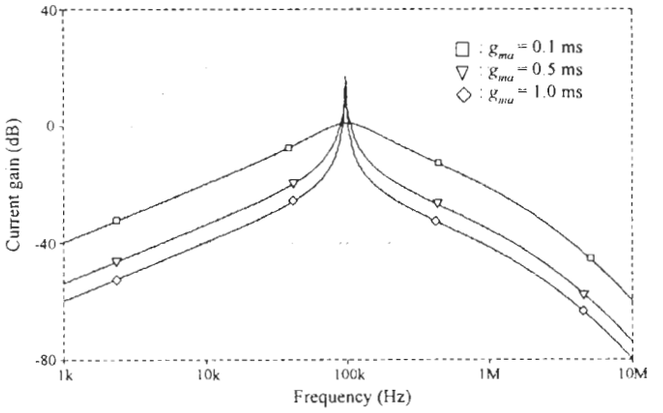

Figure19 *Simulated characteristics of bandpass filter when g_{ma} is varied*

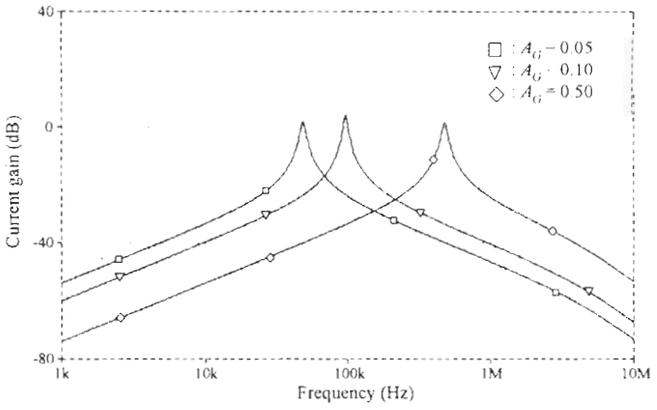

Figure 20 *Simulated characteristics of bandpass filter when A_G is varied*

Conclusions

This paper presented an approach for realizing current-mode integrator, which utilizing only two fundamental active circuit elements, i.e., a transconductance element and an internally compensated type operational amplifier, and does not require any external passive elements. By using bipolar based transconductance elements, this approach provides the possibility of tuning the current transfer function by the external controlled bias currents. Because of their active-only nature, the approach allows to realize active network functions which are suitable for implementing in monolithic integrated form in both bipolar and CMOS technologies. Since the synthesis technique utilizes an internal pole of an ICOA, it is also suitable for high frequency operation. The simulation results, which are in close agreement with the theoretical prediction, are used to verify the usefulness of the proposed design approach in current-mode operations. It should be noted that the approach based on the use of transconductance elements and ICOAs, which are the major active circuit elements in the design of g_m-C and switched capacitor circuits. In addition, many high performance and well-developed transconductance elements and ICOAs, especially in CMOS technology, are reported. Therefore, by using these elements as standard cells to implement analog signal processing circuits, this will certainly simplify the design process and the circuit is more suitable for VLSI fabrication.

References

Abuelma'atti M.T. and Alzaher. H.A. 1997. Universal three inputs and one output current-mode filter without external passive elements. **Electronics Letters.** .33: 281-283.

Higashimura. M. 1993. Current-mode lowpass and bandpass filters using operational amplifier pole. **International Journal of Electronics**. 74: 945-949.

Kardontchik.J.E. 1992. **Introduction to the Design of Transconductor-Capacitor Filters**. Boston, MA : Kluwer.

Kumar U. and Shukla. S.K. 1990. On the importance, realization experimental verification and measurements of active-R and active-C filters. **Microelectronics Journal**. 21: 21-45.

Mitra A.K. and Aatre. V.K. 1976. Low sensitivity high-frequency active R filters. **IEEE Transaction on Circuits and Systems**. 23: .670-676.

Robert G.W. and Sedra. A.S. 1992. A general class of current amplifier-based biquadratic filter circuits. **IEEE Transaction on Circuits and Systems.** 39: 257-263.

Schaumann. R. Ghausi M.S. and Laker. K.R. 1990. **Design of Analog Filters : Passive, Active RC and Switched Capacitor**. New Jersey : Prentice-Hall.

Singh A.K. and Senani. 1998. Low-component-count active-only imittances and their application in realizing simple multifunction biquads. **Electronics Letters**. 34: 718-719.

Sanchez-Sinencio. E. Geiger R.L. and Nevarez-Lozano. H. 1988. Generation of continuous-time two integrator loop OTA filter structures. **IEEE Transactions on Circuits and Systems**. 35 : 936-946.

Tsukutani. T. Higashimura. M. Sumi Y. and Fukui. Y. 2000. Electronically tunable current-mode active-only biquadratic filter. **International Journal of Electronics**. 87: 307-314.

Tsukutani. T. Higashimura. M. Sumi Y. and Fukui. Y. 2000. Voltage-mode active-only biquad. **International Journal of Electronics**. 87: 1435-1442.

Wu. J. 1994. Current-mode high-order OTA-C filters. **International Journal of Electronics**. 76 : 1115-1120.